

# HEDGEHOG/GLI-E2F1 axis modulates iASPP expression and function and regulates melanoma cell growth

S Pandolfi<sup>1,4</sup>, V Montagnani<sup>1,4</sup>, A Lapucci<sup>2</sup> and B Stecca<sup>\*1,3</sup>

HEDGEHOG (HH) signaling is a key regulator of tissue development and its aberrant activation is involved in several cancer types, including melanoma. We and others have shown a reciprocal cross talk between HH signaling and p53, whose function is often impaired in melanoma. Here we present evidence that both GLI1 and GLI2, the final effectors of HH signaling, regulate the transcription factor E2F1 in melanoma cells, by binding to a functional non-canonical GLI consensus sequence. Consistently, we find a significant correlation between *E2F1* and *PATCHED1* (*PTCH1*), *GLI1* and *GLI2* expression in human melanomas. Functionally, we find that E2F1 is a crucial mediator of HH signaling and it is required for melanoma cell proliferation and xenograft growth induced by activation of the HH pathway. Interestingly, we present evidence that the HH/GLI-E2F1 axis positively modulates the inhibitor of apoptosis-stimulating protein of p53 (iASPP) at multiple levels. HH activation induces iASPP expression through E2F1, which directly binds to *iASPP* promoter. HH pathway also contributes to iASPP function, by the induction of Cyclin B1 and by the E2F1-dependent regulation of CDK1, which are both involved in iASPP activation. Our data show that activation of HH signaling enhances proliferation in presence of E2F1 and promotes apoptosis in its absence or upon CDK1 inhibition, suggesting that E2F1/iASPP dictates the outcome of HH signaling in melanoma. Together, these findings identify a novel HH/GLI-E2F1-iASPP axis that regulates melanoma cell growth and survival, providing an additional mechanism through which HH signaling restrains p53 proapoptotic function.

*Cell Death and Differentiation* (2015) 22, 2006–2019; doi:10.1038/cdd.2015.56; published online 29 May 2015

Hedgehog (HH) signaling is a conserved pathway that directs embryonic patterning through the temporal and spatial regulation of cellular proliferation and differentiation.<sup>1,2</sup> During development, the loss of HH signaling results in severe abnormalities in mice and humans.<sup>3–5</sup> In the adult it is mostly active in stem/progenitor cells, where it regulates tissue homeostasis, repair and regeneration.<sup>6</sup> Conversely, unrestrained HH pathway activation is implicated in a variety of tumors, including those of the skin.<sup>7,8</sup> Secreted HH ligands trigger downstream signaling by binding to the transmembrane receptor Patched (PTCH1). PTCH1 relieves its inhibition on the G protein-coupled receptor Smoothed (SMO), which triggers an intracellular signaling cascade regulating the formation of the zinc finger transcription factors GLI2 and GLI3 and their translocation into the nucleus.<sup>9,10</sup> Both GLI1 and GLI2 act as main mediators of HH signaling in cancer by directly controlling the transcription of target genes, several of which are involved in proliferation.<sup>11,12</sup>

Cutaneous melanoma arises from malignant transformation of melanocytes and is the most aggressive form of skin cancer, with poor prognosis in late stages.<sup>13</sup> In contrast to other tumors, >80% of melanomas retain wild-type (wt) p53.<sup>14,15</sup>

Nevertheless, p53 tumor-suppressor activity is impaired by various mechanisms, including the deletion of the *CDKN2A* locus<sup>16,17</sup> or MDM2 and MDMX overexpression.<sup>18–21</sup> Recently, the inhibitor of apoptosis-stimulating protein of p53 (iASPP),<sup>22,23</sup> which is frequently upregulated in human cancers,<sup>24–29</sup> has been proposed to hamper p53 function in melanoma.<sup>21</sup>

HH pathway is often activated in human melanoma, where it is required for proliferation and survival both *in vitro* and *in vivo*<sup>30–32</sup> and it drives self-renewal and tumorigenicity of melanoma cancer stem cells (CSCs).<sup>33</sup> Previous data indicate a reciprocal cross talk between HH signaling and p53. Activation of the HH pathway impairs p53 function by increasing MDM2 levels.<sup>34</sup> In turn, p53 inhibits GLI1 levels, nuclear localization and transcriptional activity<sup>35</sup> and, upon DNA damage, promotes GLI1 degradation through PCAF induction.<sup>36</sup>

Restoration of wt p53 function is an attractive therapeutic approach for melanoma, and recent evidence support E2F1 as a biomarker to predict the outcome of the treatment with inhibitors of MDM2/p53 interaction.<sup>37</sup> E2F1 is a key transcriptional regulator of proliferation<sup>38–40</sup> whose aberrant activation

<sup>1</sup>Laboratory of Tumor Cell Biology, Core Research Laboratory–Istituto Toscano Tumori (CRL-ITT), Florence, Italy; <sup>2</sup>Department of Health Sciences, Section of Clinical Pharmacology and Oncology, University of Florence, Florence, Italy and <sup>3</sup>Department of Oncology, Azienda Ospedaliero-Universitaria Careggi, Florence, Italy

\*Corresponding author: B Stecca, Laboratory of Tumor Cell Biology, Core Research Laboratory–Istituto Toscano Tumori (CRL-ITT), Viale Pieraccini 6, Florence 50139 Italy; Tel: +39 055 7944567; Fax: +39 055 7944586. E-mail: barbara.stecca@ittumori.it

<sup>4</sup>These authors contributed equally to this work.

**Abbreviations:** HH, Hedgehog; PTCH1, Patched1; SMO, Smoothed; iASPP, inhibitor of apoptosis-stimulating protein of p53; CDK1, cyclin-dependent kinase 1; PIG3, p53-inducible gene 3; p53AIP1, p53-regulated apoptosis-inducing protein 1; BCL2, B-cell lymphoma 2; BCL-XL, B-cell lymphoma extra-large; CSC, cancer stem cells; GLI-BS, GLI-binding site; shRNA, short hairpin RNA; EMSA, electrophoretic mobility shift assay; JNJ, JNJ-7706621.

Received 08.10.14; revised 26.3.15; accepted 08.4.15; Edited by B Zhivotovsky; published online 29.5.15

has been described in various tumor types.<sup>41,42</sup> In melanoma E2F1 drives metastasis formation by regulating the epidermal growth factor receptor.<sup>43</sup> Notably, E2F1 has been shown to be a HH-responsive gene in cerebellar granular neural precursors, medulloblastoma and keratinocytes.<sup>44–46</sup> However, it is not known which effects induced by HH signaling activation in melanoma are mediated by E2F1. Here we demonstrate that both GLI1 and GLI2 induce E2F1 expression in melanoma by binding to the *E2F1* promoter. Importantly, we show that E2F1 dictates the outcome of HH pathway activation by controlling the expression and function of iASPP.

## Results

**HH signaling modulates E2F1 expression in melanoma cells.** To investigate whether HH pathway modulates E2F1 expression in melanoma, we inhibited HH signaling by SMO silencing, transducing patient-derived SSM2c and M26c, and commercial A375 melanoma cells with a replication-incompetent lentivirus expressing a short interference RNA targeting SMO (LV-shSMO).<sup>33</sup> Quantitative real-time PCR (qPCR) analysis showed strong reduction of mRNA levels of *SMO* and of the two HH targets *GLI1* and *PTCH1*, confirming the inhibition of HH signaling (Figure 1a). Notably, SMO silencing decreased E2F1 mRNA and protein levels compared with the control (Figures 1a and b and Supplementary Figure 1a) in all three melanoma cells. In addition, GLI2 silencing (LV-shGLI2) reduced *E2F1* mRNA levels in A375 cells, which express high levels of GLI2 (Supplementary Figures 1b and c and Supplementary Figure 2a). Conversely, activation of the HH pathway by silencing the negative regulator *PTCH1* (LV-shPTCH1; ref. 35) increased *GLI1* and *E2F1* mRNA levels (Figure 1c). Transfection of Myc-tagged GLI1 or GLI2 increased the endogenous E2F1 protein in SSM2c and M26c cells (Figures 1d and e). Altogether these results suggest that E2F1 expression in melanoma cells is affected by the modulation of the HH signaling. A publicly available microarray data set in 31 primary and 73 metastatic melanomas (GEO-46517; ref. 47) was analyzed. In support of the relevance of modulation of E2F1 by the HH pathway, a significant correlation between *E2F1* and *PTCH1*, *GLI1* and *GLI2* expression was found in metastatic melanomas, whereas in primary melanomas *E2F1* correlated only with *GLI2* (Figure 1f), suggesting an association between HH pathway activation and E2F1 expression. As a further confirm of this modulation, a significant correlation between *E2F1* and *GLI1* mRNA (Supplementary Figures 2b and c) was found in a panel of eight patient-derived melanoma cells and six melanoma cell lines (Supplementary Table 1).

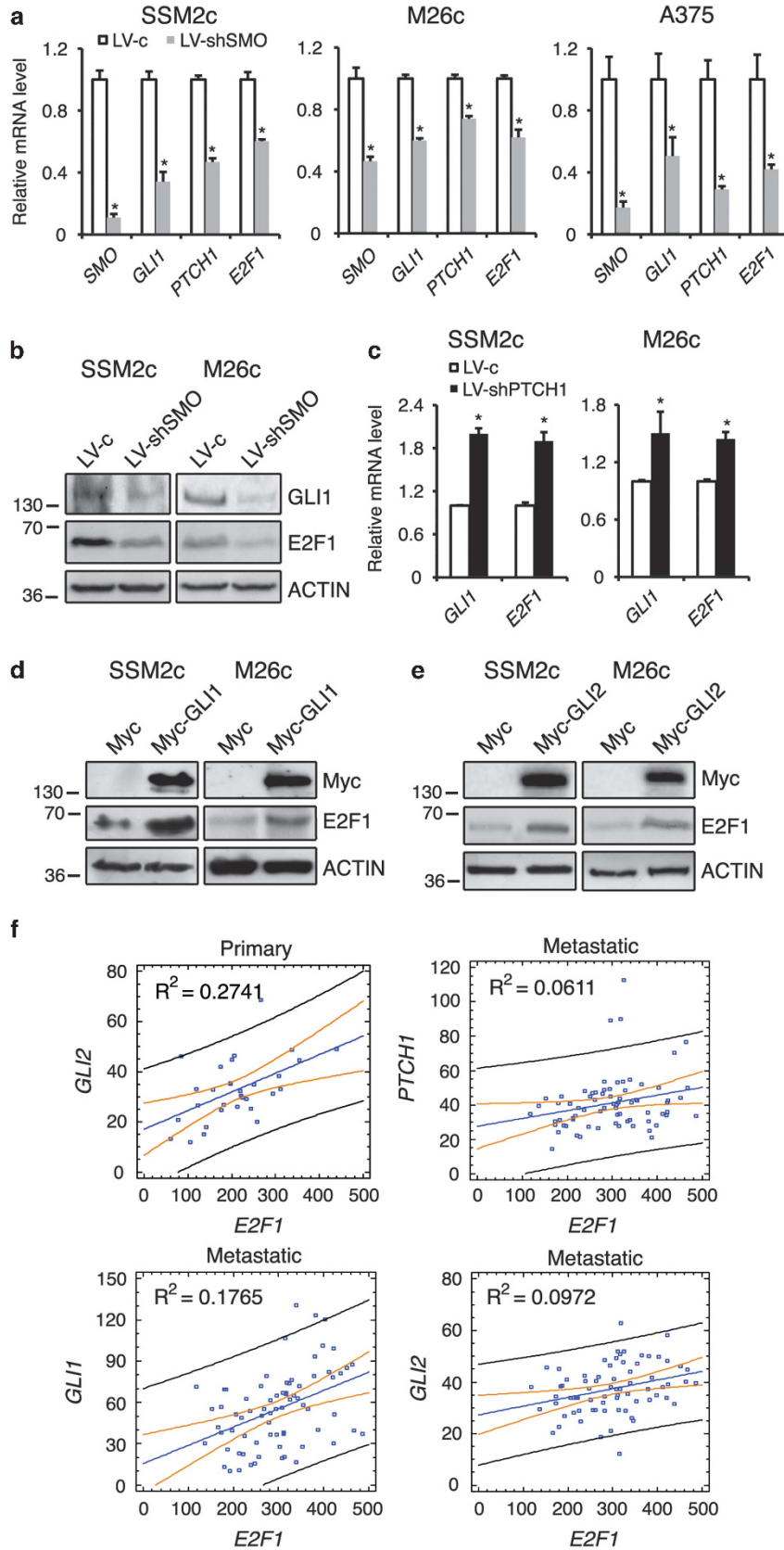
**GLI1 and GLI2 bind to a non-canonical GLI consensus sequence at *E2F1* promoter.** To test whether E2F1 expression was directly regulated by GLI1 or GLI2, we performed chromatin immunoprecipitation (ChIP) assay in M26c, SSM2c and A375 cells in which HH pathway was activated by *PTCH1* silencing. qPCR analysis on the immunoprecipitated DNA showed that both endogenous GLI1 and GLI2 bound to *E2F1* promoter (Figure 2a and Supplementary Figure 3). The activation of HH pathway

resulted in increased GLI1 binding to *PTCH1* promoter (used as positive control) in M26c and SSM2c cells, and increased GLI2 binding in A375 cells. The binding of GLI1 and GLI2 to *E2F1* promoter was not further increased by the HH pathway activation, and it was stronger than that to *PTCH1* promoter. Nevertheless, ChIP experiment showed that the activation of HH signaling increased E2F1 binding to its promoter in the proximity of a conserved E2F-binding site (Supplementary Figure 4). This suggests that the activation of the HH pathway increases E2F1 levels, which could then contribute to sustain the transactivation of its own promoter, as already shown.<sup>48</sup>

Bioinformatic analysis did not identify any canonical GLI consensus sequence (GACCACCCA)<sup>49</sup> in the *E2F1* promoter. However, GLI transcription factors are able to bind to variant GLI-binding sites (GLI-BSs) with relatively low affinity, still leading to strong transcriptional activation<sup>50,51</sup> (Figure 2b). We thus speculated that the *E2F1* promoter might contain a degenerate GLI-BS. To identify the region responsible for the modulation by GLI transcription factors, we cloned three different fragments of the *E2F1* promoter upstream of the luciferase gene (–132, –269 and –656 bp; Figure 2c). We transfected SSM2c and M26c cells with the reporter vector along with GLI1, GLI2 or E2F1, the latter used as positive control because it binds to the *E2F1* promoter close to the transcription start site.<sup>48</sup> The assay showed that both GLI1 and GLI2 transactivated the reporter driven by the –269 and –656 bp fragments, but not by the –132 bp fragment (Figure 2c). As expected, E2F1 transactivated all the three regions (Figure 2c). These results indicate the presence of a functional GLI-BS between –132 and –269 bp upstream the *E2F1* transcription start site.

To precisely map the GLI-BS, we identified two putative degenerated GLI consensus sequences (Figure 2d; site1 and site2) and we mutated each of them in two positions crucial for the efficiency of GLI-binding.<sup>50</sup> Reporter assay showed that the disruption of the site1 (Mut1) prevented the transactivation of the reporter by GLI1 and GLI2 in both SSM2c and M26c cells, whereas the mutation of the site2 (Mut2) did not have any effect (Figure 2e). Electrophoretic mobility shift assay (EMSA) in HH signaling competent murine NIH3T3 cells showed the direct binding of Gli1/2 to site1. The activation of the HH pathway by stimulation with SMO agonist SAG<sup>52</sup> led to the formation of a DNA-binding complex, which was competed with unlabeled probe. Preincubation of cell extracts with anti-GLI1 or anti-GLI2 antibodies decreased the formation of this DNA complex, suggesting the presence of Gli1 and Gli2 proteins (Figure 2f). Western blot analysis confirmed the activation of the Hh signaling upon SAG treatment (Figure 2g). Altogether these results indicate that GLI1 and GLI2 directly interact with the *E2F1* promoter by binding to a non-canonical GLI consensus sequence (CGCCTCCAG).

**E2F1 dictates the outcome of HH pathway activation in melanoma cells.** Our data indicate that in melanoma cells HH signaling directly controls the expression of E2F1, a key transcriptional regulator of proliferation.<sup>38–40</sup> We and others have previously shown that HH signaling is required for melanoma growth and stemness.<sup>30–33</sup> To investigate the effects of the HH pathway that are mediated by E2F1 in melanoma, we knocked down E2F1 after the activation of the



HH signaling. We silenced E2F1 by transducing cells with LV-shE2F1-1 and LV-shE2F1-2 lentiviruses, which strongly reduced E2F1 mRNA and protein levels (Supplementary Figures 5a and b). To investigate the presence of possible compensatory effects by other E2F members upon E2F1 silencing, we measured the expression of the activator E2F members E2F2, E2F3A and the repressor member E2F4. No significant differences were detected in E2F2, E2F3A and E2F4 expression (Supplementary Figures 5c and d) in two melanoma cells. To activate HH signaling, we silenced *PTCH1*, thus mimicking the canonical pathway activation. M26c, SSM2c and A375 cells were transduced with LV-shPTCH1 or LV-shE2F1, alone or in combination. qPCR and western blot analysis showed an increase of *GLI1*, *GLI2* and E2F1 expression upon *PTCH1* silencing, confirming the activation of the HH pathway and a strong decrease of E2F1 upon E2F1 silencing (Figure 3a and Supplementary Figure 6). To investigate the effect of E2F1 in mediating HH-induced cell growth, cells transduced as described above were seeded and allowed to grow for 7 days. In all melanoma cell lines, LV-shPTCH1 increased the cell number compared with LV-c, whereas LV-shE2F1 reduced it. Interestingly, in cells transduced with both LV-shPTCH1 and LV-shE2F1 the reduction of cell growth was greater than in cells transduced with LV-shE2F1 alone (Figure 3b).

Cytometric analysis of proliferation index (Pi) showed that HH pathway activation increased cell proliferation, as expected. E2F1 silencing by itself did not significantly affect Pi, but it markedly decreased the effect of LV-shPTCH1 (Supplementary Figures 7a and c). Cell cycle distribution did not vary, although LV-shPTCH1/LV-shE2F1-transduced cells presented a significant increase in the population with subG<sub>0</sub> DNA content, corresponding to the apoptotic fraction (Supplementary Figures 7b, d and e). Annexin V-PE/7-AAD labeling showed a consistent increase in the percentage of cells in late apoptosis when E2F1 was silenced in combination with HH signaling activation (Figure 3c). The apoptotic response observed in LV-shPTCH1/LV-shE2F1-transduced cells was consistent with the increased expression of the proapoptotic p53-target genes *PIG3* and *p53AIP1*, and decreased levels of the antiapoptotic factors *BCL-XL* and *BCL2* (Figures 3d and e and Supplementary Figure 8), suggesting the involvement of p53 in controlling cell death. Altogether these data indicate that E2F1 is critical to sustain melanoma cell growth induced by the activation of the HH signaling and suggest that E2F1 controls the balance between cell proliferation and apoptosis upon HH pathway activation.

### HH signaling regulates iASPP expression and function through E2F1.

Recent evidence indicate that melanomas

harboring wt p53 express high levels of phosphorylated iASPP, which functionally inactivates p53.<sup>21</sup> Little is known about the regulation of iASPP expression, therefore we sought to investigate whether it might be affected by the HH signaling. qPCR analysis showed that in M26c, SSM2c and A375 cells inhibition of HH pathway by SMO silencing produced a decrease of *iASPP* mRNA (Figure 4a). Conversely, activation of the HH signaling by *PTCH1* silencing resulted in *iASPP* induction (Figure 4b). Two different antibodies targeting the N- or C-terminal regions of iASPP, both validated by iASPP silencing (Supplementary Figure 9), were used to assess the impact of HH pathway activation on iASPP protein. Although we were not able to clearly detect a slow-migrating iASPP that could be compatible with the Cyclin B1/CDK1-phosphorylated form, western blot analysis showed that *PTCH1* depletion increased iASPP protein level, confirming qPCR results (Figures 4c and 5c). Because iASPP inhibits p53 function by interacting with it,<sup>21</sup> we assessed whether activation of the HH pathway might affect iASPP-p53 interaction. Indeed, in M26c and SSM2c cells transduced with LV-shPTCH1, iASPP co-immunoprecipitated p53 more efficiently than in control cells (Figure 4c), suggesting that HH signaling activation increases iASPP-p53 binding, contributing to restrain p53 function through iASPP.

Because *PTCH1* silencing, combined with E2F1 depletion, produced a marked apoptotic response with the upregulation of p53-target genes (Figures 3c, d and e and Supplementary Figure 8), we speculated that E2F1 might mediate iASPP induction upon HH signaling activation. Interrogation of publicly available databases revealed the presence of a conserved E2F-binding site within *iASPP* promoter (Supplementary Figure 10a). Indeed, ChIP analysis showed that E2F1 bound to *iASPP* promoter and that its binding was greatly increased by HH pathway activation (Figure 5a and Supplementary Figure 10b). To assess whether E2F1 mediates iASPP induction upon HH signaling activation, we performed western blot and qPCR analyses in melanoma cells transduced with LV-shPTCH1 and/or LV-shE2F1. *PTCH1* silencing induced iASPP levels in an E2F1-dependent manner, because E2F1 depletion abolished the effect of HH pathway activation (Figures 5b and c and Supplementary Figure 11). Altogether these data indicate that HH signaling modulates iASPP expression through E2F1.

The ability of iASPP to interfere with p53 function depends mainly on its phosphorylation by CDK1/Cyclin B1 complex.<sup>21</sup> We thus investigated whether HH pathway might affect also CDK1 or Cyclin B1 levels. Western blot analysis on melanoma cells transduced with LV-shPTCH1 and/or LV-shE2F1 showed that CDK1 expression was completely abolished upon E2F1 silencing (Figure 5c), consistently with a previous report

**Figure 1** HH pathway modulates the expression of E2F1 in melanoma. (a) Expression of the HH pathway components (*SMO*, *GLI1* and *PTCH1*) and *E2F1* in SSM2c, M26c and A375 cells transduced with LV-c or LV-shSMO lentiviruses, measured by quantitative PCR (qPCR). The y-axis represents the expression ratio of gene/(*EIF2α*+*HPRT* average). Data represent mean ± S.E.M. of three independent experiments. \**P* < 0.05. (b) Western blot analysis showing the decrease of endogenous *GLI1* and *E2F1* proteins upon SMO silencing in SSM2c and M26c cells.  $\beta$ -actin served as loading control. (c) Expression of *GLI1* and *E2F1* in SSM2c and M26c cells transduced with LV-c or LV-shPTCH1 lentiviruses, measured by qPCR. The y-axis represents the expression ratio of gene/(*EIF2α*+*HPRT* average). Data represent mean ± S.E.M. of three independent experiments. \**P* < 0.05. (d,e) Western blot analysis showing an increase of endogenous *E2F1* protein upon Myc-tagged *GLI1* (d) or Myc-tagged *GLI2* (e) overexpression in SSM2c and M26c cells.  $\beta$ -actin served as loading control. (f) Positive correlation between the levels of *E2F1* and *GLI2* in primary melanomas ( $R^2 = 0.2741$ ,  $P = 0.0025$ ), *E2F1* and *PTCH1* ( $R^2 = 0.0611$ ,  $P = 0.0351$ ), *GLI1* ( $R^2 = 0.1765$ ,  $P = 0.0002$ ) and *GLI2* ( $R^2 = 0.0972$ ,  $P = 0.0072$ ) transcripts in metastatic melanomas

indicating that E2F1 regulates CDK1 expression.<sup>53</sup> ChIP analysis revealed a strong enrichment of E2F1 on the *CDK1* promoter (Figure 5d and Supplementary Figure 12), supporting a direct regulation,<sup>54</sup> and the binding was further increased upon HH pathway activation. PTCH1 depletion also increased Cyclin B1 levels, as previously reported<sup>55,56</sup> and this increase was independent of E2F1, because it occurred also in cells transduced with LV-shPTCH1/LV-shE2F1 (Figure 5c). These data indicate that HH signaling contributes to both iASPP induction, through E2F1, and to iASPP function, via Cyclin B1 and E2F1-dependent regulation of CDK1.

HH signaling contributes to iASPP function through E2F1-dependent regulation of CDK1 (Figure 5). Therefore we speculated that the inhibition of CDK1 activity with the CDK1 inhibitor JNJ-7706621 (JNJ, 500 nM),<sup>57</sup> which was recently shown to block iASPP phosphorylation,<sup>21</sup> would mimic the effect of E2F1 depletion. JNJ treatment markedly reduced the ability of iASPP to co-immunoprecipitate p53 (Figure 6a), confirming the efficacy of CDK1 inhibition. Growth assay showed that JNJ treatment produced a stronger reduction in the cell number of melanoma cells with activated HH pathway compared with the control (Figure 6b), paralleling the results obtained by the E2F1 silencing (Figure 3b). Cytometric analysis revealed that cells with activated HH signaling were more sensitive to CDK1 inhibition than the control cells, undergoing increased apoptosis and cell death upon JNJ treatment (Figures 6c and d). Altogether these data show that the inhibition of CDK1 activity produces the similar increase of apoptosis as E2F1 depletion in cells with activated HH pathway, suggesting that E2F1 determines the outcome of HH signaling activation by controlling not only iASPP expression but also its function through CDK1.

**Depletion of E2F1 suppresses HH-mediated melanoma xenograft growth.** To investigate whether E2F1 regulates HH-induced growth of melanoma xenografts *in vivo*, M26c cells stably transduced with LV-c, LV-shPTCH1 and/or LV-shE2F1 were engrafted subcutaneously into athymic-nude mice. Activation of HH signaling resulted in almost two-fold larger xenografts than the control cells (Figures 7a, b and c), confirming that the activation of HH pathway increases melanoma cell growth *in vivo*.<sup>33,58</sup> E2F1 silencing reduced

of about 50% the size of melanoma xenografts compared with LV-c and strongly reduced the increase of tumor growth induced by PTCH1 silencing (Figures 7a and c). Western blot analysis in tumors dissected 42 days after injection confirmed the increase of E2F1 levels induced by HH pathway activation and its reduction upon E2F1 silencing (Figure 7d), consistently with the tumor growth curve. The difference in xenograft growth between LV-shE2F1 and LV-shPTCH1/LV-shE2F1 was not significant as we documented *in vitro*. To explain this result, we investigated whether E2F1 depletion in a context of HH activation might affect the self-renewal of melanoma CSC grown as spheres.<sup>33,59</sup> We found that E2F1 silencing markedly reduced the ability of melanoma CSCs to form secondary spheres, suggesting that it might be involved in controlling stemness. The effect of HH pathway activation was reduced by E2F1 silencing to the level of LV-c. However, even in absence of E2F1, PTCH1 silencing was still able to increase CSC self-renewal, suggesting that the regulation of melanoma stemness by HH signaling is only partially dependent on E2F1 (Supplementary Figure 13). Nevertheless, western blot analysis on xenografts showed the same iASPP, Cyclin B1 and CDK1 pattern obtained *in vitro* (Figures 4d and 5c), suggesting that the HH/GLI-E2F1-iASPP axis contributes to regulate the melanoma cell growth *in vivo*.

## Discussion

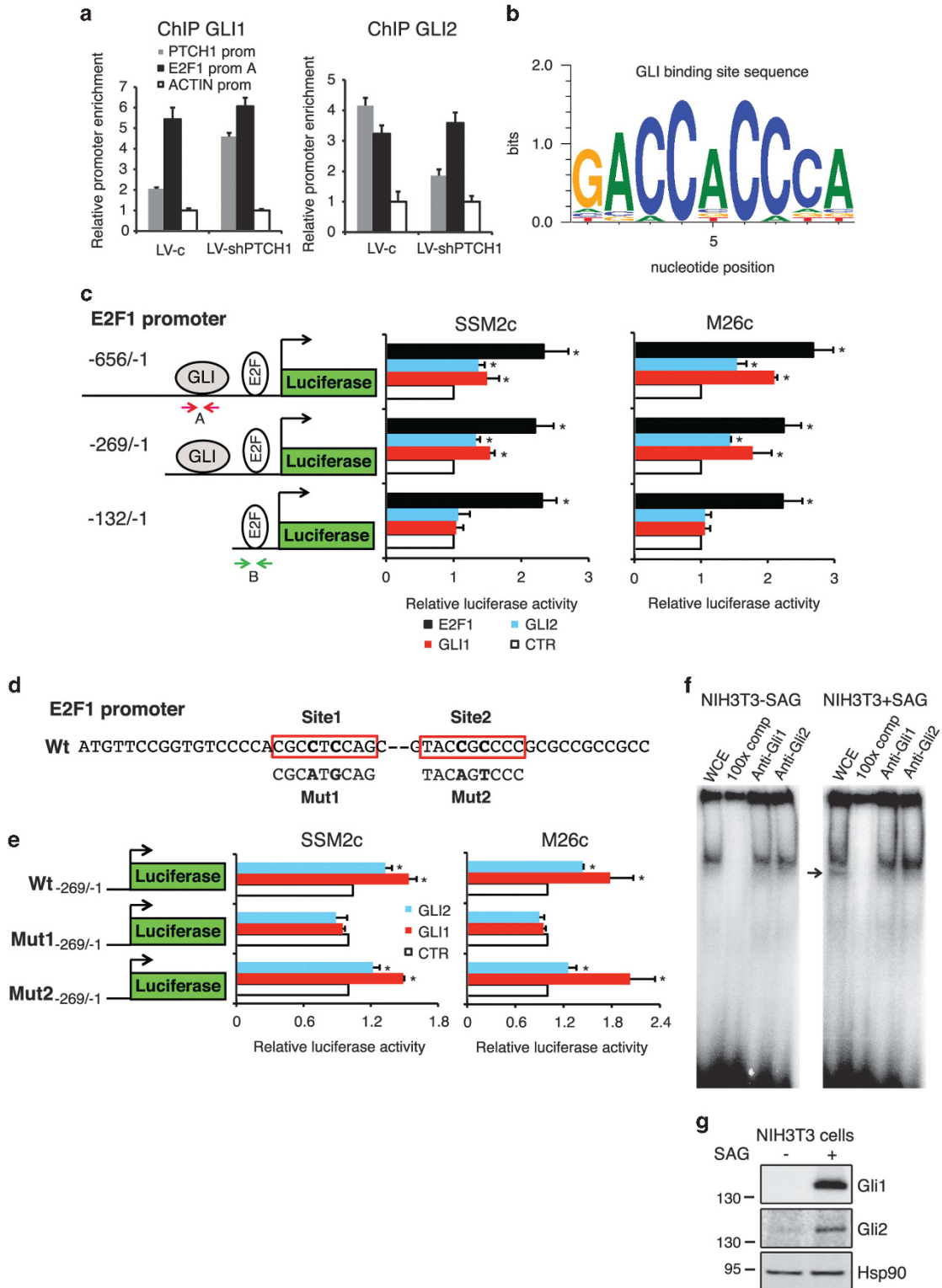
Here we define a novel HH/GLI-E2F1-iASPP axis that regulates melanoma cell growth and identify E2F1 as a central player in determining the outcome of HH signaling, by controlling the levels and function of the p53 inhibitor iASPP (Figure 8).

Previous data indicated that E2F1 is induced in response to SHH stimulation<sup>44,45</sup> and by GLI2 overexpression.<sup>46</sup> Nevertheless, there are no evidence indicating a direct regulation. Here we show that the HH pathway directly regulates E2F1 expression in melanoma cells and that GLI1 and GLI2 bind to and transactivate the *E2F1* promoter. Although bioinformatic analysis did not find any canonical GLI consensus sequence in *E2F1* promoter, we identified a functional non-canonical GLI-BS (CGCCTCCAG) by site-directed mutagenesis. This

**Figure 2** GLI1 and GLI2 bind to *E2F1* promoter. (a) Chromatin immunoprecipitation (ChIP) assay showing that both endogenous GLI1 and GLI2 bind to *PTCH1* and *E2F1* promoters in M26c cells transduced with LV-c or LV-shPTCH1. The y-axis represents the relative promoter enrichment, normalized on the input material. *ACTIN* promoter was used as negative control and set to 1. (b) Consensus GLI DNA-binding motif calculated from experimentally validated GLI-binding sites<sup>50</sup> using WebLogo3.<sup>65</sup> Positions 4C and 6C are essential for DNA binding, whereas all the other positions allow a certain degree of sequence variation. (c) Quantification of dual-luciferase reporter assay in SSM2c and M26c cells showing that GLI1 and GLI2 transactivate *E2F1* promoter in a region between -132 bp and -269 bp from the transcription start site. Three fragments of different length (132, 269 and 656 bp) of *E2F1* promoter were assayed for their ability to be transactivated by GLI1 or GLI2; E2F1 was used as a positive control. The red and green arrows mark the positions of the primers used in ChIP, described in Supplementary Figure 4. Relative luciferase activities were firefly/*Renilla* ratios, with the level induced by control equated to 1. The data represent mean  $\pm$  S.E.M. of at least five independent experiments. *P*-values are as follows: -656 bp: CTR versus GLI1, *P* = 0.0214 in SSM2c; *P* = 0.0007 in M26c; CTR versus GLI2, *P* = 0.0013 in SSM2c; *P* = 0.0182 in M26c; -269 bp: CTR versus GLI1, *P* < 0.0001 in SSM2c; *P* = 0.0183 in M26c; CTR versus GLI2, *P* < 0.0001 in SSM2c; *P* = 0.0006 in M26c; CTR versus E2F1, *P* < 0.04 in -132, -269 and -656 bp, in both the cells. (d) Putative GLI-binding sites (site1 and site2) in the -269 bp *E2F1* promoter that were mutagenized (Mut1 and Mut2). Note that both the positions essential for DNA binding (4C and 6C) were mutagenized. (e) Quantification of dual-luciferase reporter assay in SSM2c and M26c cells showing that mutagenesis of Mut1, but not Mut2 site, prevented GLI1 and GLI2 from transactivating the -269 bp fragment of the *E2F1* promoter. Relative luciferase activities were firefly/*Renilla* ratios, with the level induced by the control equated to 1. Data represent mean  $\pm$  S.E.M. of at least five independent experiments. (f) Electrophoretic mobility shift assays of site1 in *E2F1* promoter. In the right panel the arrow indicates the specific DNA complex that appears upon SAG treatment in NIH3T3 cells. Competition was carried out using a 100-fold excess of unlabeled site1 oligonucleotide. Disruption of the complex is achieved with preincubation of the WCE with anti-Gli1 and anti-Gli2 antibodies. WCE, whole-cell extract; 100x comp, unlabeled site1 competitor. (g) Western blot analysis showing the increase of endogenous Gli1 and Gli2 proteins upon SAG treatment (100 nM, 48 h) in NIH3T3 cells. Hsp90 served as loading control

site matches the minimal GLI-BS requirements,<sup>50</sup> and indeed mutation of two essential cytosines in the 4th and 6th position completely abolishes the ability of GLI1 and GLI2 to transactivate the *E2F1* promoter. Despite the divergence from the canonical GLI-BS, EMSA analysis confirmed the binding

of GLI1/2 to this site, in agreement with the reporter assay. The biological relevance of this modulation is supported by a significant positive correlation between the expression of *E2F1* and of the HH pathway components (*GLI1*, *GLI2* and *PTCH1*) in human melanomas (Figure 1f) and in a set of



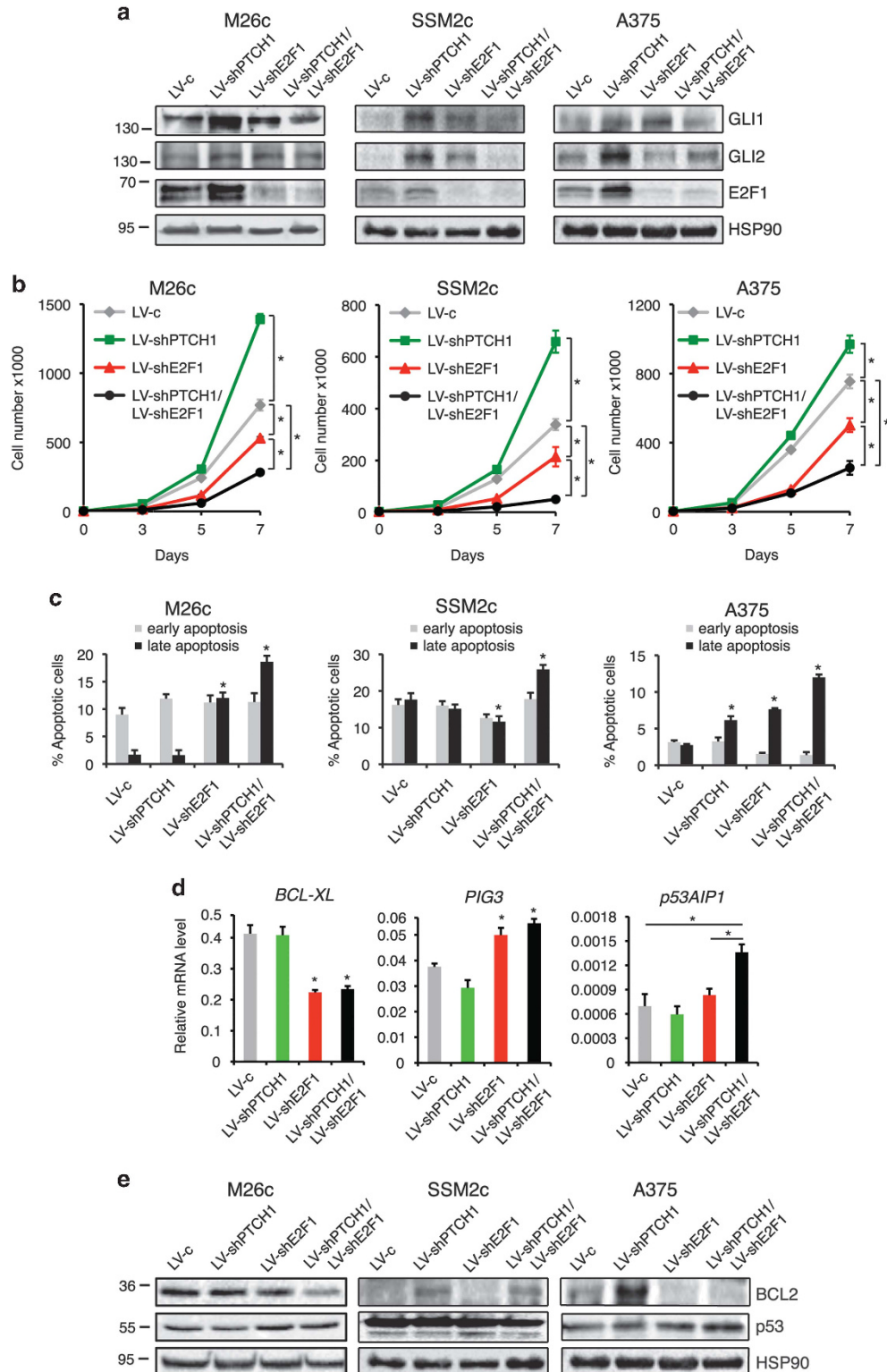


**Figure 3** E2F1 is required for the increase in melanoma cell growth induced by activation of the HH signaling. **(a)** Western blot analysis of GLI1, GLI2 and E2F1 in M26c, SSM2c and A375 cells transduced with the indicated lentiviruses. HSP90 served as loading control. **(b)** Growth curve in M26c, SSM2c and A375 cells transduced with the indicated lentiviruses, showing that E2F1 silencing abolishes melanoma cell growth induced by activation of the HH pathway. The data represent mean  $\pm$  S.E.M. of three independent experiments.  $*P < 0.05$ . **(c)** Annexin V-PE/7-AAD labeling of M26c, SSM2c and A375 cells transduced with the indicated lentiviruses, showing a marked increase of the late-apoptotic fraction in cells transduced with LV-shE2F1 and with LV-shPTCH1/LV-shE2F1 lentiviruses compared with the control (LV-c). No differences in the early apoptosis are observed. The data represent mean  $\pm$  S.E.M. of three independent experiments.  $*P < 0.05$ . **(d)** Quantitative PCR analysis of *BCL-XL*, *PIG3* and *p53AIP1* expression in M26c cells transduced with the indicated lentiviruses. The y-axis represents expression ratio of gene/(*EIF2 $\alpha$* +*HPRT* average). Data represent mean  $\pm$  S.E.M. of three independent experiments.  $*P < 0.05$ . **(e)** Western blot analysis of BCL2 and p53 in M26c, SSM2c and A375 cells transduced with the indicated lentiviruses. HSP90 served as loading control

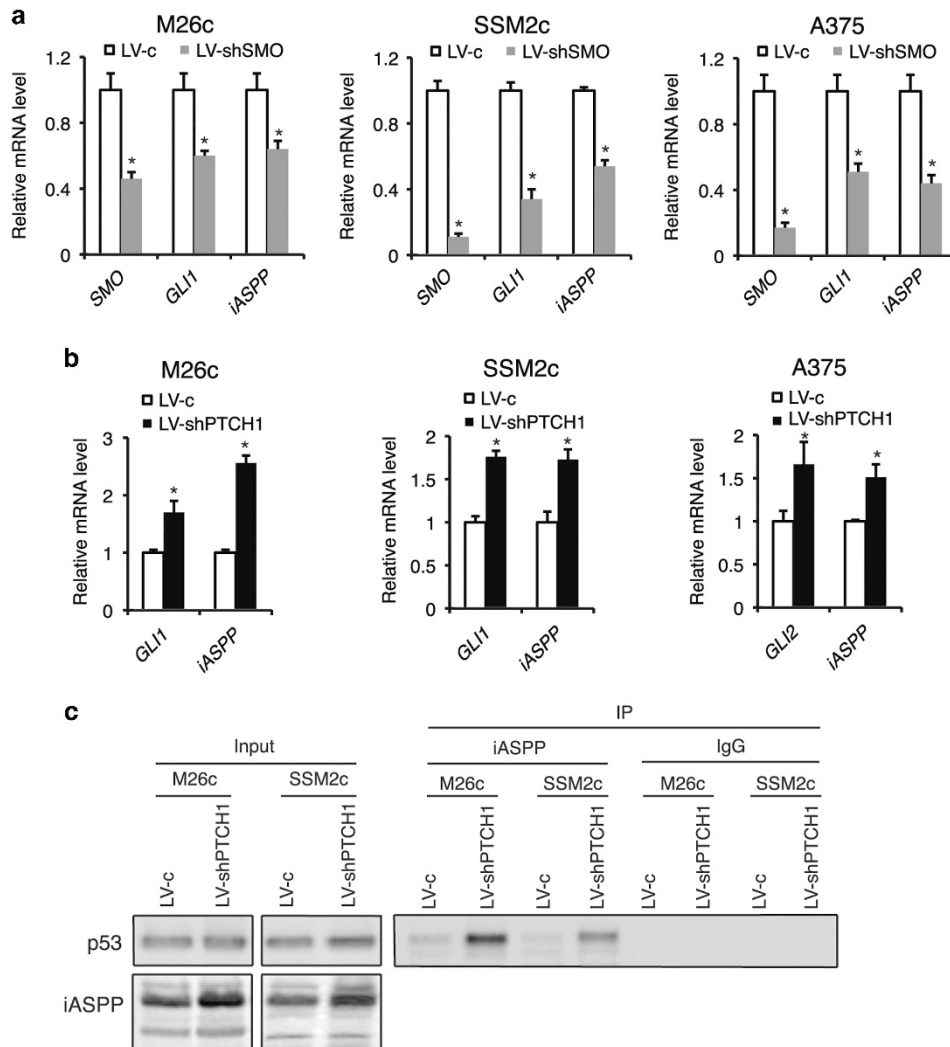


**Figure 4** HH pathway modulates iASPP expression and function in melanoma cells. **(a)** Expression of *SMO*, *GLI1* and *iASPP* in M26c, SSM2c and A375 cells transduced with LV-c or LV-shSMO lentiviruses, measured by quantitative PCR (qPCR). The y-axis represents the expression ratio of gene/(*EIF2 $\alpha$* +*HPRT* average). Data represent mean  $\pm$  S.E.M. of three independent experiments. \* $P < 0.05$ . **(b)** Expression of *GLI1* and *iASPP* in M26c, SSM2c and A375 cells transduced with LV-c or LV-shPTCH1 lentiviruses, measured by qPCR. The y-axis represents the expression ratio of gene/(*EIF2 $\alpha$* +*HPRT* average). Data represent mean  $\pm$  S.E.M. of three independent experiments. \* $P < 0.05$ . **(c)** Co-immunoprecipitation to determine the binding between endogenous iASPP and p53 in M26c and SSM2c cells transduced with LV-c or LV-shPTCH1 lentiviruses. Cell lysates are labeled as input

commercial and primary melanoma cells (Supplementary Figure 2).

We previously showed that HH signaling regulates proliferation and survival of human melanoma and melanoma CSCs.<sup>30,33</sup> E2F1 is a key regulator of cell cycle and survival and it is often upregulated or hyperactivated in a variety of tumors, including melanoma.<sup>41,42</sup> Our data confirm the role of HH pathway and E2F1 in regulating melanoma cell growth. Interestingly, the activation of HH signaling in the absence of E2F1 *in vitro* produces a marked apoptotic response and reduces melanoma growth more than E2F1 depletion alone. Multiple evidence indicate that activation of HH signaling leads to the inhibition of the tumor-suppressor p53,<sup>34,35</sup> which is itself a negative modulator of GLI1.<sup>35</sup> Although HH activation promotes cell proliferation, enhanced GLI1 levels are associated with markers of DNA replication stress.<sup>35</sup> As a consequence, the inhibition of p53 function contributes both

to fuel the HH activation and to blunt the stress response.<sup>35</sup> Here we identify the HH/GLI-E2F1-iASPP axis as a novel mechanism of p53 inhibition in response to HH signaling. In this context, E2F1 plays a crucial role in determining the balance between proliferation and apoptosis in response to HH pathway activation through the regulation of iASPP.

Although iASPP is overexpressed in a variety of human cancers,<sup>24–29</sup> little is known about the regulation of its expression. Here we find that the activation of HH signaling increases iASPP expression in melanoma cells. The induction is mediated by E2F1, which binds to the *iASPP* promoter in a region closed to a conserved E2F-binding site; notably, the activation of HH signaling increases E2F1 binding to *iASPP* promoter, consistently with the presence of a HH-E2F1-iASPP axis. A previous report showed that the ability of iASPP to inhibit p53 depends on its phosphorylation by Cyclin B1/CDK1 complex.<sup>21</sup> Our data indicate that HH signaling contributes to

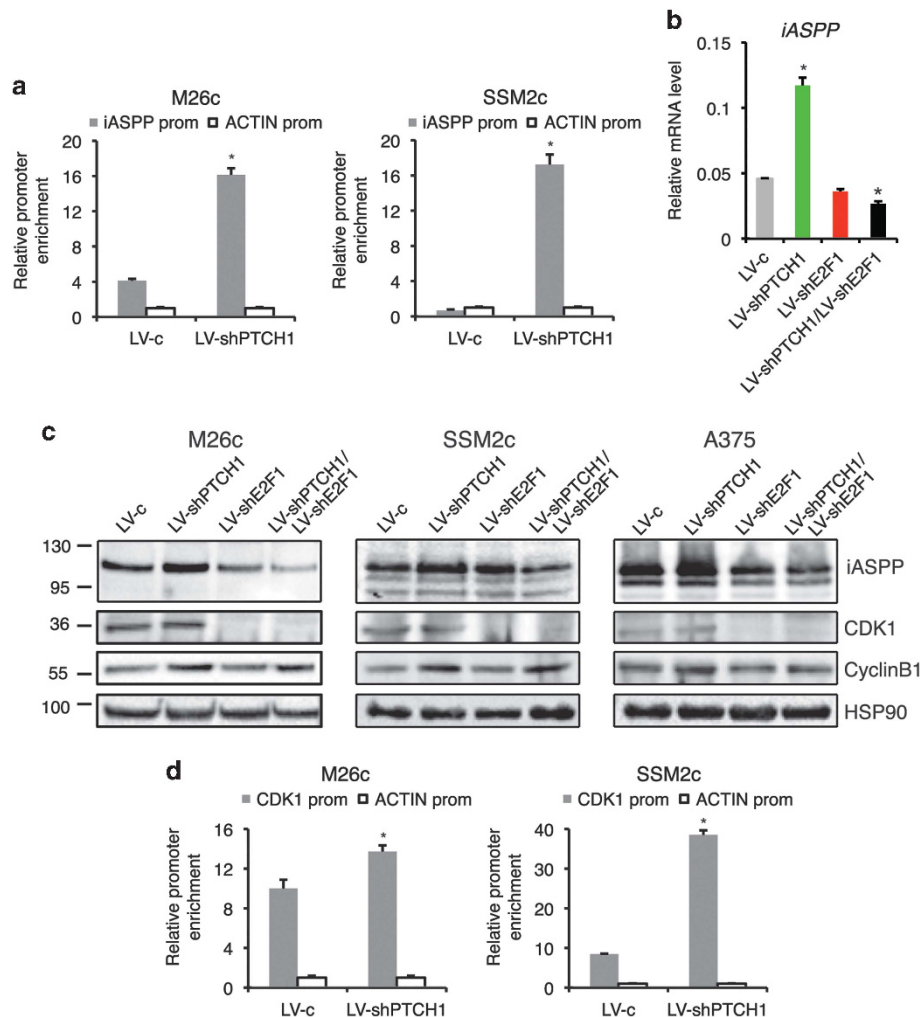


**Figure 5** E2F1 mediates the modulation of iASPP by HH pathway in melanoma cells. (a) Chromatin immunoprecipitation (ChIP) assay showing that endogenous E2F1 binds to *iASPP* promoter in M26c and SSM2c cells transduced with LV-c or LV-shPTCH1. The y-axis represents the relative promoter enrichment, normalized on input material. *ACTIN* promoter was used as negative control and set to 1. (b) Quantitative PCR analysis of *iASPP* expression in M26c cells transduced with the indicated lentiviruses. The y-axis represents the expression ratio of gene/(*EIF2 $\alpha$* +*HPRT* average). Data represent mean  $\pm$  S.E.M. of three independent experiments. \* $P < 0.05$ . (c) Western blot analysis of iASPP, CDK1 and Cyclin B1 in M26c, SSM2c and A375 cells transduced with indicated lentiviruses. iASPP was detected using an N-terminal Ab in M26c cells and a C-terminal Ab in SSM2c and A375 cells. HSP90 served as loading control. (d) ChIP assay showing that endogenous E2F1 binds to *CDK1* promoter in M26c and SSM2c cells transduced with LV-c or LV-shPTCH1 lentiviruses. The y-axis represents the relative promoter enrichment, normalized on input material. *ACTIN* promoter was used as negative control and set to 1

the regulation of iASPP function also at post-translational level, by controlling both the Cyclin B1 and CDK1 levels and favouring its interaction with p53. Activation of HH pathway increases Cyclin B1 expression,<sup>55,56</sup> and this modulation is independent from E2F1. In addition, HH signaling regulates CDK1 expression through E2F1,<sup>53</sup> which increases its binding to *CDK1* promoter upon HH signaling activation (Figure 5).

We show that E2F1 is an important mediator of HH signaling *in vivo*, because its depletion abolishes the increase in tumor growth induced by the activation of the HH pathway. We do not find significant difference between LV-shE2F1 and LV-shPTCH1/LV-shE2F1 xenografts. This is likely due to other downstream effectors of HH pathway (e.g. stemness factors)<sup>59</sup> that *in vivo* might favor CSC self-renewal independently from E2F1, thus contributing to tumor growth, as suggested by the self-renewal experiments. Nevertheless, as a confirmation of the relevance of our findings, western blot analysis on

xenografts reproduces a similar pattern of iASPP, Cyclin B1 and CDK1 expression observed *in vitro*.

Reactivation of the endogenous wt p53 has been proposed as a parallel strategy along with targeted therapy to suppress melanoma growth more efficiently.<sup>60–62</sup> The HH/GLI-E2F1-iASPP axis (Figure 8) described in this study provides novel targets for the therapeutic intervention for melanomas and possibly other tumors harboring wt p53 and with activated HH pathway. Our data show that E2F1 depletion in the context of activated HH pathway restores p53 apoptotic function. The fact that treatment with JNJ-7706621, a CDK1 inhibitor<sup>57</sup> that prevents iASPP activation,<sup>21</sup> produces the same effect in terms of cell growth and apoptosis as E2F1 silencing, confirms the relevance of the HH-E2F1-iASPP axis we show in this study. Therefore, blockade of iASPP activity through interference with E2F1 function or by CDK1 inhibition, is predicted to restore the tumor-suppressive effects of p53, turning the

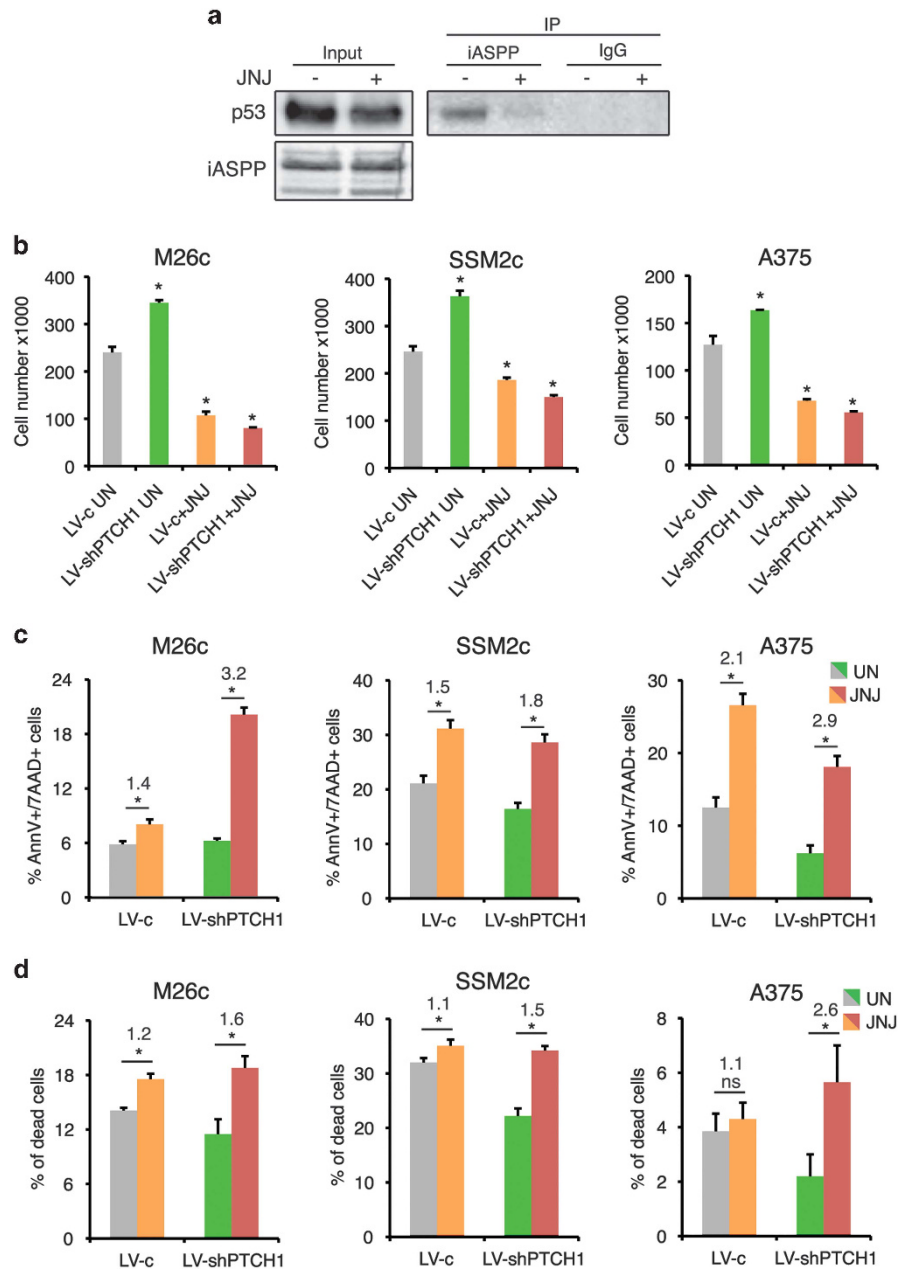


**Figure 6** Inhibition of CDK1 mimics silencing of E2F1 upon HH pathway activation. (a) Co-immunoprecipitation to determine the binding between endogenous iASPP and p53 in M26c control cells and treated with 500 nM JNJ-7706621 (JNJ) for 16 h. Cell lysates are labeled as input. (b) Cell growth assay in M26c, SSM2c and A375 cells transduced with LV-c or LV-shPTCH1 lentiviruses after treatment with the CDK1 inhibitor JNJ-7706621 for 72 h (500 nM). The data represent mean  $\pm$  S.E.M. of three independent experiments. \* $P < 0.05$ . (c) Annexin V-PE+/7-AAD+ (late apoptotic) cells in M26c, SSM2c and A375 cells transduced with LV-c or LV-shPTCH1 lentiviruses after treatment with the CDK1 inhibitor JNJ-7706621 for 48 h (500 nM). The data represent mean  $\pm$  S.E.M. of three independent experiments. \* $P < 0.05$ . Fold changes are indicated. (d) Evaluation of cell death by propidium iodide staining of M26c, SSM2c and A375 cells transduced with LV-c or LV-shPTCH1 lentiviruses after treatment with the CDK1 inhibitor JNJ-7706621 for 48 h (500 nM). The data represent mean  $\pm$  S.E.M. of three independent experiments. \* $P < 0.05$ . Fold changes are indicated. UN, untreated cells. Note that cells with activated HH signaling are more sensitive to CDK1 inhibition

proliferative activity of HH signaling into an apoptotic response.

#### Materials and methods

**Patient samples and cell cultures.** HEK-293T (CRL-11268), NIH3T3 (CRL-1658) and A375 (CRL-1619) cell lines were obtained from ATCC (Manassas, VA, USA). SSM2c and M26c patient-derived melanoma cells were previously described.<sup>33,58</sup> Human melanoma specimens (Supplementary Table 1) were

obtained after approved protocols by the local Ethics Committee. In brief, fresh tissue samples were digested enzymatically using 1 mg/ml collagenase A and 20  $\mu$ g/ml DNase I (Roche Diagnostic, Mannheim, Germany) and grown in DMEM supplemented with 10% fetal bovine serum, 1% Penicillin-streptomycin, 2 mM L-Glutamine (Lonza, Basel, Switzerland). The identity of melanoma cells was verified by immunocytochemistry using anti-Melan A, anti-S100 and anti-Vimentin antibodies, as previously described.<sup>33</sup> Mycoplasma was periodically tested by 4',6-diamidino-2-phenylindole inspection and PCR. Direct sequencing revealed that both SSM2c and M26c cells harbor wt p53 with codon 72 Proline polymorphism.<sup>58</sup> A375

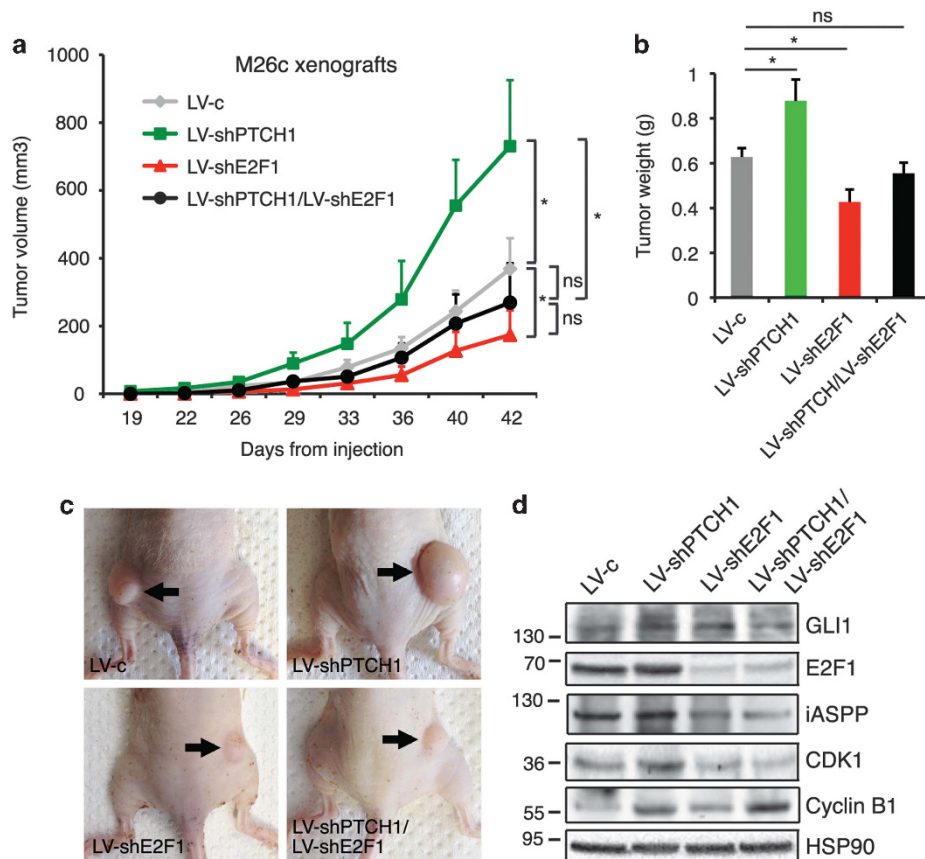


**Figure 7** E2F1 silencing prevents HH-induced melanoma xenograft growth. (a) M26c cells transduced with LV-c, LV-shPTCH1, LV-shE2F1 or LV-shPTCH1/LV-shE2F1 lentiviruses were injected subcutaneously in athymic-nude mice. Quantification of tumor volume ( $n = 12$  per group), showing that E2F1 silencing prevented the increase of tumor growth induced by the activation of the HH signaling.  $*P < 0.05$ . (b) Tumor weight of xenografts, as indicated.  $*P < 0.05$ . (c) Representative images of M26c xenografts, as indicated. (d) Western blot analysis of GLI1, E2F1, iASPP, CDK1 and Cyclin B1 in tumors derived from M26c xenografts. iASPP was detected using an N-terminal Ab. HSP90 served as loading control

melanoma cells harbor wt p53. For growth curve 3000 cells/well were plated in 12-well plates and counted on days 3–5–7. For growth assay after JNJ treatment 15 000 cells/well were plated in 12-well plates and treated with the CDK1 inhibitor JNJ-7706621 (500 nM, JNJ; Merck, Darmstadt, Germany) for 72 h. Puromycin was used at 2  $\mu$ g/ml to select for transduced cells.

**Plasmids, cloning, mutagenesis and lentiviral vectors.** Vectors used for overexpression were: pCS2+MT (Addgene, Cambridge, MA, USA), pCMV-E2F1 (kind gift from M. Chiariello),<sup>63</sup> Myc-tagged human GLI1 (pCS2+MT-GLI1, kind gift from A. Ruiz i Altaba)<sup>35</sup> and GLI2 (pCS2+MT-GLI2, Addgene).<sup>5</sup> Three fragments of E2F1 promoter (–132, –269 and –656 bp) were PCR amplified with Platinum Pfx DNA polymerase (Life Technologies, Carlsbad, CA, USA) and cloned in pGL3Basic vector (Promega, Madison, WI, USA) using NheI-XhoI sites, to generate –132/–269/–656 bp-E2F1 prom-luc reporters. Primers used were: E2F1 prom –132 bp, FW, 5'-ACGCTAGCGCGGTAAAGCCAATAGG-3'; E2F1 prom –269 bp, FW, 5'-ACGCTAGCATGTTCCGGTGTCCAC-3'; E2F1 prom –656 bp, FW, 5'-ACGCTAGCTAGTGAGGAATGAATG-3'; E2F1 prom, RV, 5'-ACCTGAGATCCTTTTGC CGCGAAA-3'. Mutations of E2F1 prom –269-bp reporter were introduced using QuickChange II (Agilent Technologies, Santa Clara, CA, USA) with the following oligos: Mut1, FW, 5'-GGTGTCCCCACGCATGCAGCCAGGGGACG-3'; Mut1, RV, 5'-CGTCCCTGGCTGCATGCGTGGGACACC-3'; Mut2, FW, 5'-GCCATTGGCCGTACAGTCCCGCGCCGCGCC-3'; Mut2, RV, 5'-GGCGCGCGCGCGGACTGTACGCGCAATGGC-3'. Plasmid identity was verified by direct sequencing. All transfections were performed in OptiMEM (Life Technologies) using X-tremeGENE transfection reagent (Roche Diagnostic) according to the manufacturer's protocol. Lentiviruses were produced in HEK-293T cells. Lentiviral vectors pLV-CTH (LV-c), pLV-CTH-shPTCH1 (LV-shPTCH1)<sup>35</sup> and pLKO.1-puro-

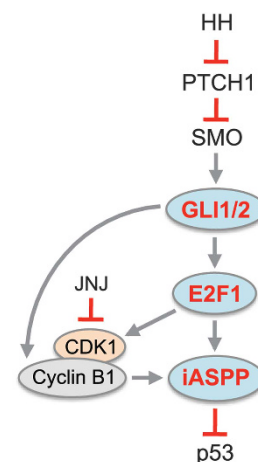


**Figure 8** Model of the HH/GLI-E2F1-iASPP axis. E2F1 is a direct target of GLI1 and GLI2, and acts downstream of HH signaling by controlling the expression and activation of iASPP. E2F1 regulates iASPP expression and CDK1 expression. The effectors of HH signaling GLI1 and GLI2 regulate Cyclin B1 expression. The complex CDK1/Cyclin B1 phosphorylates iASPP and increases its ability to bind and inactivate p53. JNJ-7706621 (JNJ) is a CDK1 inhibitor

shSMO (LV-shSMO)<sup>33</sup> were previously described. pLKO.1-puro (LV-c), pLKO.1-puro-shE2F1-1 (LV-shE2F1-1); targeting sequence 5'-GACCTCTCGACTGTGACTTT-3', exon 7) were from Open Biosystems (Lafayette, CO, USA). Most experiments were performed with LV-shE2F1-1.

**Luciferase reporter assay.** E2F1 prom-luc reporters (-132/-269/-656 bp) were used in combination with *Renilla* luciferase pRL-TK reporter vector (Promega) to normalize luciferase activities; pGL3Basic vector (Promega) was used to equal DNA amounts. Luminescence was measured using the Dual-Glo Luciferase Assay System (Promega) and the GloMax 20/20 Luminometer (Promega).

**Electrophoretic mobility shift assay.** NIH3T3 cells were treated with 100 nM SAG for 48 h to activate the HH pathway, harvested and lysed in lysis buffer (20 mM HEPES pH 7.9, 25% glycerol, 0.5% Nonidet P-40, 420 mM NaCl, 1.5 mM MgCl<sub>2</sub>, 0.2 mM EDTA, 1 mM DTT) to obtain whole-cell extracts (WCE).<sup>64</sup> To analyze the binding of Gli proteins to Site1 at E2F1 promoter we used the following oligonucleotide and its complementary strand: site1F, 5'-AGCTACCTGGAGCGCTCT-3'; site1R, 5'-TCGAAGACGCCTCCAGGGT-3'. The DNA-binding reaction was performed by incubating 20 fmol of double-stranded <sup>32</sup>P-labeled oligo with 40 μg of WCE in a total volume of 20 μl containing 1 μg poly-dC, 100 mM KCl in 40 mM HEPES (pH 7.9), 10 mM MgCl<sub>2</sub>, 0.4 mM EDTA, 4 mM DTT and 40% glycerol<sup>64</sup> for 20 min at room temperature. In indicated competition experiments, a 100-fold excess of unlabeled oligo was used. When using antibodies, proteins were preincubated with anti-GLI1 (N-16, Santa Cruz Biotechnology, Santa Cruz, CA, USA) or anti-GLI2 (#AF3635, R&D Systems, Minneapolis, MN, USA) antibodies for 20 min at room temperature before adding the radiolabeled probe. The samples were separated on native polyacrylamide gel (6% polyacrylamide:bisacrylamide, 29:1) at 4 °C for 3 h and the signal was detected by Cyclone Storage Phosphor System (Perkin Elmer, Waltham, MA, USA).

**Western blot and co-immunoprecipitation.** Samples were lysed in ice in RIPA buffer (1% NP-40, 150 mM NaCl, 5 mM EDTA, 0.25% NaDOC, 50 mM Tris-HCl pH 7.5, SDS 0.1%) added with protease and phosphatase inhibitors, sonicated to shear DNA and centrifuged at 14000 r.p.m. for 20 min at 4 °C; supernatant was collected as WCE. For co-immunoprecipitation experiments 700 μg WCE were diluted with IP buffer (0.5% NP-40, 100 mM NaCl, 5 mM EDTA, 10% glycerol, 50 mM Tris-HCl pH 7.5) added with protease and phosphatase inhibitors to a final volume of 450 μl and incubated overnight at 4 °C with Dynabeads Protein G (Life Technologies) pre-conjugated with anti-iASPP antibody (49.3, Santa Cruz Biotechnology) or irrelevant IgG (Life Technologies). Beads were washed three times with IP buffer, proteins were eluted with Laemmli buffer and visualized on SDS polyacrylamide gel electrophoresis. The following antibodies were used for western blot: rabbit anti-iASPP (ab34898), (Abcam, Cambridge, United Kingdom), rabbit anti-E2F1 (#3742), rabbit anti-BCL2 (#2976), mouse anti-GLI1 (L42B10) (Cell Signaling Technology, Danvers, MA, USA), goat anti-GLI2 (#AF3635; R&D Systems), mouse anti-Myc (9E10), mouse anti-HSP90 (F-8), mouse anti-p53 (DO-1), mouse anti-iASPP (2808C5a), rabbit anti-CDK1 (C-19), rabbit anti-Cyclin B1 (H-433; Santa Cruz Biotechnology), mouse anti-β-ACTIN (AC-15; Sigma-Aldrich, St. Louis, MO, USA). Chemiluminescent detection was used.

**Quantitative real-time PCR.** Total RNA from adherent cells was isolated with TriPure Isolation Reagent (Roche Diagnostics). After DNase I treatment (Roche Diagnostics), RNA was subjected to reverse transcription with High Capacity cDNA Reverse Transcription Kit (Life Technologies). qPCRs were carried out at 60 °C using FastStart SYBR Green Master (Roche Diagnostic) in a Rotorgene-Q (Qiagen, Hilden, Germany). Primer sequences are the following (5' to 3'): GLI1-F, 5'-CCCAGTACATGCTGGTGGTT-3' and GLI1-R, 5'-GCTTTACTGCAGCCCTCGT-3'; PTCH1-F, 5'-GGCAGCGGTAGTAGTGGTGTTC-3' and PTCH1-R, 5'-TGTAGC GGGTATTGCTGTGTG-3'; SMO-F 5'-GGGAGGCTACTTCCATCC-3' and SMO-R 5'-GGCAGCTGAAGGTAATGAGC-3'; E2F1-F, 5'-GCTGAGCCACTCGG CTGACG-3'; E2F1-R, 5'-CACTGGTGTGGCTGCC-3'; iASPP-F, 5'-AGCCT TAAAGAGACAGGACGG-3'; iASPP-R, 5'-TGTTTCATGGCCAGCGACT-3'; BCL-XL-F, 5'-GGTAACTGGGGTGCATTG-3'; BCL-XL-R, 5'-GCTGCTGCATTGTT CCCATAG-3'; PIG3-F, 5'-CTGAACCGGGCGGACTTAAT-3'; PIG3-R, 5'-GTGTCCC CGATCTCCAGTG-3'; p53AIP1-F, 5'-CTCGGTGATGCTCCGAATG-3'; p53AIP1-R, 5'-GGCCTGGAGAGACTAGACC-3'. Primers for human reference genes are: EIF2a-F, 5'-GGATGGGACCTTGTTCCT-3' and EIF2a-R, 5'-CCACGTTGCCA

GGACAGTAT-3'; HPRT-F, 5'-GCCAGACTTTGTGGATTG-3' and HPRT-R, 5'-CTCTCATCTTAGGCTTTGATTTTG-3'.

**Chromatin immunoprecipitation.** Melanoma cells were fixed with 1% formaldehyde for 10 min and fixation was stopped by adding 125 mM glycine for 5 min. Cells were harvested and lysed in Cell Lysis Buffer (5 mM PIPES pH 8, 85 mM KCl, 0.5% NP-40) added with protease inhibitors. Nuclei were collected by centrifugation and lysated in nuclear lysis buffer (1% SDS, 10 mM EDTA, 50 mM Tris-HCl pH 8) added with protease inhibitors. Chromatin was sonicated to an average size of 300–500 bp using a SONOPULS Mini20 Sonicator (Bandelin, Berlin, Germany) equipped with a cuphorn and diluted with ChIP Dilution Buffer (1.8% Triton X-100, 2 mM EDTA, 300 mM NaCl); input material was collected. Chromatin was incubated overnight with Dynabeads Protein G (Life Technologies) pre-conjugated with anti-GLI1 (N-16; Santa Cruz Biotechnology), anti-GLI2 (#AF3635, R&D Systems) or anti-E2F1 (#3742; Cell Signaling Technology) antibodies. Immunocomplexes were washed with low salt wash buffer (20 mM Tris-HCl, pH 8, 2 mM EDTA, 150 mM NaCl, 0.1% SDS, 1% Triton X-100), high salt wash buffer (20 mM Tris-HCl, pH 8, 2 mM EDTA, 500 mM NaCl, 0.1% SDS, 1% Triton X-100) and LiCl wash buffer (250 mM LiCl, 1% NP-40, 1 mM EDTA, 10 mM Tris-HCl, pH 8, 1% sodium deoxycholate) and twice with TE (1 mM EDTA, 10 mM Tris-HCl, pH 8). All the solutions were added with 1X complete Protease Inhibitor Cocktail (Roche Diagnostic). DNA was eluted with 1% SDS at 85 °C for 10 min, crosslinks were reversed overnight at 65 °C with 200 mM NaCl. After treatment with 4 μg RNaseA (Life Technologies) at 37 °C for 30 min and with 20 μg Proteinase K (Roche Diagnostic) at 60 °C for 2 h, the DNA was recovered by using the QIAquick PCR Purification Kit (Qiagen). qPCR were carried out at 60 °C using FastStart SYBR Green Master (Roche Diagnostic) in a Rotorgene-Q (Qiagen). Primers used were: E2F1promA-F, 5'-CTATAGAAGGTCAGTGGGATGC-3' and E2F1promA-R, 5'-AGGCTTTGTCCGGATGGTA-3'; PTCH1prom-F, 5'-ACACACTGGGTGCTACC-3' and PTCH1prom-R, 5'-CTGTGATGCTGGCTGGGTTT-3'; iASPPprom-F, 5'-GGAG AAATAGGGGCAATCCGT-3' and iASPPprom-R, 5'-GCATGAGACTAAACCCCGA-3'; CDK1prom-F, 5'-TCGCTCCGCTCAATTTCC-3' and CDK1prom-R, 5'-GGGCT ACCCGATTGGTGAAT-3'; ACTInprom-F, 5'-TCGAGCCATAAAGGCAACT-3' and ACTInprom-R, 5'-CTTCTCAATCTCGCTCTCG-3'.

**Flow cytometry analysis.** Apoptosis was assessed by cytometric analysis of Annexin V/7-AAD labeled cells using Annexin V-PE/7-AAD apoptosis kit (Becton Dickinson, Franklin Lakes, NJ, USA), according to manufacturer's protocol. Cell death was measured by propidium iodide staining; cells were incubated with 100ng/ml PI for 5 min before analysis. Cytometric analysis was performed with FACS-Canto II (Becton Dickinson).

**Cell sorting, nude mice and xenografts.** Melanoma cells were transduced with either pLV-CTH (LV-c) or pLV-CTH-shPTCH1 (LV-shPTCH1) lentiviruses. Cells transduced with LV-c or LV-shPTCH1 also express green fluorescent protein (GFP) and were FACS (fluorescent-activated cell sorter)-sorted with the BD FACS-Aria cell sorter (Becton Dickinson). GFP-positive cells were then transduced with either pLKO.1-puro (LV-c) or pLKO.1-puro-shE2F1-1 (LV-shE2F1) lentiviruses and selected for puromycin resistance. For xenotransplantation M26c cells were resuspended in Matrigel (Becton Dickinson)/DMEM (1/1) and inoculated subcutaneously in lateral flanks of adult female athymic-nude mice (Foxn1 nu/nu; Harlan Laboratories, Udine, Italy; 40 000 cells/injection). Animals were housed in SPF conditions and monitored daily. Subcutaneous tumor size was measured twice a week with a caliper. Tumor volumes were calculated using the formula:  $V = W^2 \times L \times 0.5$ , where  $W$  and  $L$  are, respectively, tumor width and length. The experiment was approved by the Italian Ministry of Health and was in accordance with the Italian guidelines and regulations.

**Statistical analysis.** The data represent mean ± S.E.M. values and are calculated on at least 3–5 independent experiments.  $P$ -values were calculated using Student's  $t$ -test. A two-tailed value of  $P < 0.05$  was considered statistically significant.

**Bioinformatic analysis.** Publicly available gene expression data for a series of 31 primary and 73 metastatic melanomas were profiled on Affymetrix U133 platform (Gene Expression Omnibus GEO-46517).<sup>47</sup> To assess the relationship between *E2F1*, *PTCH1*, *GLI1* and *GLI2* expression we performed Pearson's correlation and simple regression analysis using StatGraphics Centurion XVI software (Statpoint Technologies).

**Conflict of Interest**

The authors declare no conflict of interest.

**Acknowledgements.** We thank Gianni Del Sal (ICGEB, Trieste, Italy), Silvia Pietrobono, Roberta Santini, Maria Rivero and Alessandro Apollo (Tumor Cell Biology Unit, ITT, Florence) for helpful comments on the paper and discussion. We are grateful to Lorenzo Borgognoni, Gianni Gerlini (S. Maria Annunziata Hospital, Florence, Italy), Nicola Pimpinelli (Department of Dermatology, University of Florence, Florence, Italy) and Riccardo Gattai (Department of Medical-Surgical Critical Area, General and Oncological Surgery, University of Florence, Florence, Italy) for providing samples and Laura Polisenio (Istituto Toscano Tumori, Pisa, Italy) for providing SK-Mel-2, SK-Mel-5, SK-Mel-28 and 501Mel melanoma cell lines. This work was supported by grants from AIRC (Associazione Italiana per la Ricerca sul Cancro; IG-9566 and IG-14184), Regional Health Research Program 2009 and Fondazione Cassa di Risparmio di Firenze (2011.1072, FiorGen Foundation) to BS.

- Ingham PW, McMahon AP. Hedgehog signaling in animal development: paradigms and principles. *Genes Dev* 2002; **15**: 3059–3087.
- Ruiz i Altaba A Hedgehog-Gli signaling in Human Diseases. Plenum, 2006.
- Chiang C, Litingtung Y, Lee E, Young KE, Corden JL, Westphal H et al. Cyclopia and defective axial patterning in mice lacking Sonic hedgehog gene function. *Nature* 1996; **383**: 407–413.
- Belloni E, Muenke M, Roessler E, Traverso G, Siegel-Bartelt J, Frumkin A et al. Identification of Sonic hedgehog as a candidate gene responsible for holoprosencephaly. *Nat Genet* 1996; **14**: 353–356.
- Roessler E, Ermilov AN, Grange DK, Wang A, Grachtchouk M, Dlugosz AA et al. A previously unidentified amino-terminal domain regulates transcriptional activity of wild-type and disease-associated human GLI2. *Hum Mol Genet* 2005; **14**: 2181–2188.
- Beachy PA, Karhadkar SS, Berman DM. Tissue repair and stem cell renewal in carcinogenesis. *Nature* 2004; **432**: 324–331.
- Teglund S, Toftgård R. Hedgehog beyond medulloblastoma and basal cell carcinoma. *Biochim Biophys Acta* 2010; **1805**: 181–208.
- Pandolfi S, Stecca B. Cooperative integration between HEDGEHOG-GLI signalling and other oncogenic pathways: implications for cancer therapy. *Expert Rev Mol Med* 2015; **17**: e5.
- Rohatgi R, Scott MP. Patching the gaps in Hedgehog signalling. *Nat Cell Biol* 2007; **9**: 1005–1009.
- Jiang J, Hui CC. Hedgehog signaling in development and cancer. *Dev Cell* 2008; **15**: 801–812.
- Oliver TG, Grasfeder LL, Carroll AL, Kaiser C, Gillingham CL, Lin SM et al. Transcriptional profiling of the Sonic hedgehog response: a critical role for N-myc in proliferation of neuronal precursors. *Proc Natl Acad Sci USA* 2003; **100**: 7331–7336.
- Milla LA, Arros A, Espinoza N, Remke M, Kool M, Taylor MD et al. Neogenin1 is a Sonic Hedgehog target in medulloblastoma and is necessary for cell cycle progression. *Int J Cancer* 2014; **134**: 21–31.
- Balch CM, Gershenwald JE, Soong SJ, Thompson JF, Atkins MB, Byrd DR et al. Final version of 2009 AJCC melanoma staging and classification. *J Clin Oncol* 2009; **27**: 6199–6206.
- Straume O, Akslen LA. Alterations and prognostic significance of p16 and p53 protein expression in subgroups of cutaneous melanoma. *Int J Cancer* 1997; **74**: 535–539.
- Hodis E, Watson IR, Kryukov GV, Arold ST, Imielinski M, Theurillat JP et al. A landscape of driver mutations in melanoma. *Cell* 2012; **150**: 251–263.
- Curtin JA, Fridlyand J, Kageshita T, Patel HN, Busam KJ, Kutzner H et al. Distinct sets of genetic alterations in melanoma. *N Engl J Med* 2005; **353**: 2135–2147.
- Zhang Y, Xiong Y, Yarbrough WG. ARF promotes MDM2 degradation and stabilizes p53: ARF-INK4a locus deletion impairs both the Rb and p53 tumor suppression pathways. *Cell* 1998; **92**: 725–734.
- Gembaraska A, Luciani F, Fedele C, Russell EA, Dewaele M, Villar S et al. MDM4 is a key therapeutic target in cutaneous melanoma. *Nat Med* 2012; **18**: 1239–1247.
- Muthusamy V, Hobbs C, Nogueira C, Cordon-Cardo C, McKee PH, Chin L et al. Amplification of CDK4 and MDM2 in malignant melanoma. *Genes Chromosomes Cancer* 2006; **45**: 447–454.
- Polsky D, Melzer K, Hazan C, Panageas KS, Busam K, Drobniak M et al. HDM2 protein overexpression and prognosis in primary malignant melanoma. *J Natl Cancer Inst* 2002; **94**: 1803–1806.
- Lu M, Breysens H, Salter V, Zhong S, Hu Y, Baer C et al. Restoring p53 function in human melanoma cells by inhibiting MDM2 and cyclin B1/CDK1-phosphorylated nuclear iASPP. *Cancer Cell* 2013; **23**: 618–633.
- Bergamaschi D, Samuels Y, O'Neil NJ, Trigiante G, Crook T, Hsieh JK et al. 2003 iASPP oncoprotein is a key inhibitor of p53 conserved from worm to human. *Nat Genet* 2003; **33**: 162–167.
- Bergamaschi D, Samuels Y, Sullivan A, Zvelebil M, Breysens H, Bisso A et al. iASPP preferentially binds p53 proline-rich region and modulates apoptotic function of codon 72-polymorphic p53. *Nat Genet* 2006; **38**: 1133–1141.
- Zhang X, Wang M, Zhou C, Chen S, Wang J. The expression of iASPP in acute leukemias. *Leuk Res* 2005; **29**: 179–183.
- Saebø M, Skjelbred CF, Nexø BA, Wallin H, Hansteen IL, Vogel U et al. Increased mRNA expression levels of ERCC1, OGG1 and RAI in colorectal adenomas and carcinomas. *BMC Cancer* 2006; **6**: 208–214.
- Liu Z, Zhang X, Huang D, Liu Y, Zhang X, Liu L et al. Elevated expression of iASPP in head and neck squamous cell carcinoma and its clinical significance. *Med Oncol* 2012; **29**: 3381–3388.
- Chen J, Xie F, Zhang L, Jiang WG. iASPP is over-expressed in human non-small cell lung cancer and regulates the proliferation of lung cancer cells through a p53 associated pathway. *BMC Cancer* 2010; **10**: 694.
- Cao L, Huang Q, He J, Lu J, Xiong Y. Elevated expression of iASPP correlates with poor prognosis and chemoresistance/radioresistance in FIGO lb1-IIa squamous cell cervical cancer. *Cell Tissue Res* 2013; **352**: 361–369.
- Morris EV, Cerundolo L, Lu M, Verrill C, Fritzsche F, White MJ et al. Nuclear iASPP may facilitate prostate cancer progression. *Cell Death Dis* 2014; **5**: e1492.
- Stecca B, Mas C, Clement V, Zbinden M, Correa R, Piguat V et al. Melanomas require HEDGEHOG-GLI signaling regulated by interactions between GLI1 and the RAS-MEK/AKT pathways. *Proc Natl Acad Sci USA* 2007; **104**: 5895–5900.
- Jalili A, Mertz KD, Romanov J, Wagner C, Kalthoff F, Stuetz A et al. NVP-LDE225, a potent and selective SMOOTHENED antagonist reduces melanoma growth in vitro and in vivo. *PLoS One* 2013; **8**: e69064.
- O'Reilly KE, de Miera EV, Segura MF, Friedman E, Polisenio L, Han SW et al. Hedgehog pathway blockade inhibits melanoma cell growth in vitro and in vivo. *Pharmaceuticals* 2013; **6**: 1429–1450.
- Santini R, Vinci MC, Pandolfi S, Penachioni JY, Montagnani V, Olivito B et al. Hedgehog-GLI signaling drives self-renewal and tumorigenicity of human melanoma-initiating cells. *Stem Cells* 2012; **30**: 1808–1818.
- Abe Y, Oda-Sato E, Tobiuma K, Kawachi K, Taya Y, Okamoto K et al. Hedgehog signaling overrides p53-mediated tumor suppression by activating Mdm2. *Proc Natl Acad Sci USA* 2008; **105**: 4838–4843.
- Stecca B, Ruiz i Altaba A. A GLI1-p53 inhibitory loop controls neural stem cell and tumour cell numbers. *EMBO J* 2009; **28**: 663–676.
- Mazzà D, Infante P, Colicchia V, Greco A, Alfonsi R, Siler M et al. PCAF ubiquitin ligase activity inhibits Hedgehog/Gli1 signaling in p53-dependent response to genotoxic stress. *Cell Death Differ* 2013; **20**: 1688–1697.
- Verhaegen M, Checinska A, Riblett MB, Wang S, Soengas MS. E2F1-dependent oncogenic addiction of melanoma cells to MDM2. *Oncogene* 2012; **31**: 828–841.
- Huang Y, Ishiko T, Nakada S, Utsugisawa T, Kato T, Yuan ZM. Role for E2F in DNA damage-induced entry of cells into S phase. *Cancer Res* 1997; **57**: 3640–3643.
- Müller H, Helin K. The E2F transcription factors: key regulators of cell proliferation. *Biochim Biophys Acta* 2000; **1470**: M1–12.
- Wu L, Timmers C, Maiti B, Saavedra HI, Sang L, Chong GT et al. The E2F1-3 transcription factors are essential for cellular proliferation. *Nature* 2001; **414**: 457–462.
- Halaban R, Cheng E, Smicun Y, Germino J. Deregulated E2F transcriptional activity in autonomously growing melanoma cells. *J Exp Med* 2000; **191**: 1005–1016.
- Nelson MA, Reynolds SH, Rao UN, Goulet AC, Feng Y, Beas A et al. Increased gene copy number of the transcription factor E2F1 in malignant melanoma. *Cancer Biol Ther* 2006; **5**: 407–412.
- Alla V, Engelmann D, Niemetz A, Pahnke J, Schmidt A, Kunz M et al. E2F1 in melanoma progression and metastasis. *J Natl Cancer Inst* 2010; **102**: 127–133.
- Bhatia B, Hsieh M, Kenney AM, Nahlé Z. Mitogenic Sonic hedgehog signaling drives E2F1-dependent lipogenesis in progenitor cells and medulloblastoma. *Oncogene* 2011; **30**: 410–422.
- Bhatia B, Potts CR, Guldal C, Choi S, Korshunov A, Pfister S et al. Hedgehog-mediated regulation of PPAR $\gamma$  controls metabolic patterns in neural precursors and shh-driven medulloblastoma. *Acta Neuropathol* 2012; **123**: 587–600.
- Regl G, Kasper M, Schnidar H, Eichberger T, Neill GW, Philpott MP et al. Activation of the BCL2 promoter in response to Hedgehog/GLI signal transduction is predominantly mediated by GLI2. *Cancer Res* 2004; **64**: 7724–7731.
- Kabbarah O, Nogueira C, Feng B, Nazarian RM, Bosenberg M, Wu M et al. Integrative genome comparison of primary and metastatic melanomas. *PLoS One* 2010; **5**: e10770.
- Johnson DG, Ohtani K, Nevins JR. Autoregulatory control of E2F1 expression in response to positive and negative regulators of cell cycle progression. *Genes Dev* 1994; **8**: 1514–1525.
- Kinzler KW, Vogelstein B. The GLI gene encodes a nuclear protein which binds specific sequences in the human genome. *Mol Cell Biol* 1990; **10**: 634–642.
- Winklmayr M, Schmid C, Laner-Plamberger S, Kaser A, Aberger F, Eichberger T et al. Non-consensus GLI binding sites in Hedgehog target gene regulation. *BMC Mol Biol* 2010; **11**: 2.
- Peterson KA, Nishi Y, Ma W, Vedenko A, Shokri L, Zhang X et al. Neural-specific Sox2 input and differential Gli-binding affinity provide context and positional information in Shh-directed neural patterning. *Genes Dev* 2012; **26**: 2802–2816.
- Chen JK, Taipale J, Young KE, Maiti T, Beachy PA. Small molecule modulation of Smoothed activity. *Proc Natl Acad Sci USA* 2002; **99**: 14071–14076.

53. Wu J, Kharebava G, Piao C, Stoica BA, Dinizo M, Sabirzhanov B *et al*. Inhibition of E2F1/CDK1 pathway attenuates neuronal apoptosis in vitro and confers neuroprotection after spinal cord injury in vivo. *PLoS One* 2012; **7**: e42129.
54. Konishi Y, Bonni A. The E2F-Cdc2 cell-cycle pathway specifically mediates activity deprivation-induced apoptosis of postmitotic neurons. *J Neurosci* 2003; **23**: 1649–1658.
55. Eichberger T, Sander V, Schnidar H, Regl G, Kasper M, Schmid C *et al*. Overlapping and distinct transcriptional regulator properties of the GLI1 and GLI2 oncogenes. *Genomics* 2006; **87**: 616–632.
56. Locker M, Agathocleous M, Amato MA, Parain K, Harris WA, Perron M. Hedgehog signaling and the retina: insights into the mechanisms controlling the proliferative properties of neural precursors. *Genes Dev* 2006; **20**: 3036–3048.
57. Emanuel S, Rugg CA, Gruninger RH, Lin R, Fuentes-Pesquera A, Connolly PJ *et al*. The in vitro and in vivo effects of JNJ-7706621: a dual inhibitor of cyclin-dependent kinases and aurora kinases. *Cancer Res* 2005; **65**: 9038–9046.
58. Pandolfi S, Montagnani V, Penachioni JY, Vinci MC, Olivito B, Borgognoni L *et al*. WIP1 phosphatase modulates the Hedgehog signaling by enhancing GLI1 function. *Oncogene* 2013; **32**: 4737–4747.
59. Santini R, Pietrobono S, Pandolfi S, Montagnani V, D'Amico M, Penachioni JY *et al*. SOX2 regulates self-renewal and tumorigenicity of human melanoma-initiating cells. *Oncogene* 2014; **33**: 4697–4708.
60. Jochemsen AG. Reactivation of p53 as therapeutic intervention for malignant melanoma. *Curr Opin Oncol* 2014; **26**: 114–119.
61. Lu M, Miller P, Lu X. Restoring the tumour suppressive function of p53 as a parallel strategy in melanoma therapy. *FEBS Lett* 2014; **588**: 2616–2621.
62. Qiu S, Cai Y, Gao X, Gu SZ, Liu ZJ. A small peptide derived from p53 linker region can resume the apoptotic activity of p53 by sequestering iASPP with p53. *Cancer Lett* 2015; **356**: 910–917.
63. Melillo RM, Helin K, Lowy DR, Schiller JT. Positive and negative regulation of cell proliferation by E2F-1: influence of protein level and human papillomavirus oncoproteins. *Mol Cell Biol* 1994; **14**: 8241–8249.
64. Agren M, Kogerman P, Kleman MI, Wessling M, Toftgård R. Expression of the PTCH1 tumor suppressor gene is regulated by alternative promoters and a single functional Gli-binding site. *Gene* 2004; **330**: 101–114.
65. Crooks GE, Hon G, Chandonia JM, Brenner SE. WebLogo: a sequence logo generator. *Genome Res* 2004; **14**: 1188–1190.



This work is licensed under a Creative Commons Attribution-NonCommercial-ShareAlike 4.0 International License. The images or other third party material in this article are included in the article's Creative Commons license, unless indicated otherwise in the credit line; if the material is not included under the Creative Commons license, users will need to obtain permission from the license holder to reproduce the material. To view a copy of this license, visit <http://creativecommons.org/licenses/by-nc-sa/4.0/>

Supplementary Information accompanies this paper on Cell Death and Differentiation website (<http://www.nature.com/cdd>)